PRESSURE TEST ON THE VIKING LANDER CAPSULE AT MACH NUMBER 10

E. C. Knox, et al

Arnold Engineering Development Center
Arnold Air Force Station, Tennessee

December 1972

AEDC-TR-72-185

PRESSURE TEST ON THE VIKING LANDER CAPSULE AT MACH NUMBER 10

E. C. Knox and J. T. Best, Jr.

ARO, Inc.

December 1972

Approved for public release; distribution unlimited.

VON KÁRMÁN GAS DYNAMICS FACILITY
ARNOLD ENGINEERING DEVELOPMENT CENTER
AIR FORCE SYSTEMS COMMAND
ARNOLD AIR FORCE STATION, TENNESSEE

31

NOTICES

When U. S. Government drawings specifications, or other data are used for any purpose other than a definitely related Government procurement operation, the Government thereby incurs no responsibility nor any obligation whatsoever, and the fact that the Government may have formulated, furnished, or in any way supplied the said drawings, specifications, or other data, is not to be regarded by implication or otherwise, or in any manner licensing the holder or any other person or corporation, or conveying any rights or permission to manufacture, use, or sell any patented invention that may in any way be related thereto.

Qualified users may obtain copies of this report from the Defense Documentation Center.

References to named commercial products in this report are not to be considered in any sense as an endorsement of the product by the United States Air Force or the Government.

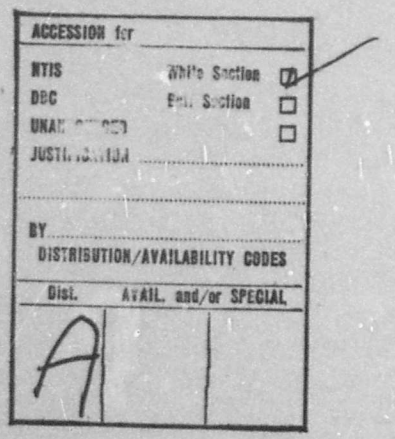

UNCLASSIFIED

Security Classification

DOCUMENT CONTROL DATA - R & D

(Security classification of title, body of abstract and indexing annotation must be entered when the overall report is classified)

1 ORIGINATING ACTIVITY (Corporate author) Arnold Engineering Development Center Arnold Air Force Station, Tennessee 37389	2a. REPORT SECURITY CLASSIFICATION UNCLASSIFIED 2b. GROUP N/A

3 REPORT TITLE

PRESSURE TEST ON THE VIKING LANDER CAPSULE AT MACH NUMBER 10

4 DESCRIPTIVE NOTES (Type of report and inclusive dates)

Final Report - July 10 and 11, 1972

5 AUTHOR(S) (First name, middle initial, last name)

E. C. Knox and J. T. Best, Jr., ARO, Inc.

6 REPORT DATE December 1972	7a. TOTAL NO. OF PAGES 33	7b. NO. OF REFS 3
8a. CONTRACT OR GRANT NO. b. PROJECT NO c. Program Element 921E-5 d.	9a. ORIGINATOR'S REPORT NUMBER(S) AEDC-TR-72-185 9b. OTHER REPORT NO(S) (Any other numbers that may be assigned this report) ARO-VKF-TR-72-158	

10 DISTRIBUTION STATEMENT

Approved for public release; distribution unlimited.

11 SUPPLEMENTARY NOTES Available in DDC	12. SPONSORING MILITARY ACTIVITY NASA Langley Research Center Hampton, Virginia 23365

13 ABSTRACT

Surface pressure tests were made on a 0.0873-scale model of the Viking Lander Capsule at Mach number 10 and Reynolds numbers, based on the model aeroshell radius, of 0.28×10^6 and 0.79×10^6. Angle of attack was varied from -26 to 26 deg with yaw angles of -5 and -10 included at the capsule estimated trim angle of attack of 11.2 deg. Results show little effect of protuberances representing a camera bump, an antenna, a reaction control system, and other appendages on the base cover pressure distribution. Comparisons with data from another test facility are also presented.

Ia

DD FORM 1 NOV 65 1473

UNCLASSIFIED

Security Classification

14. KEY WORDS	LINK A		LINK B		LINK C	
	ROLE	WT	ROLE	WT	ROLE	WT
Viking Lander Capsule						
pressure distribution						
aircraft protuberances						
hypersonic flow						
wind tunnel tests						

AFSC
Arnold AFS Tenn

Ib

PRESSURE TEST ON THE VIKING LANDER CAPSULE AT MACH NUMBER 10

E. C. Knox and J. T. Best, Jr.
ARO, Inc.

TC

FOREWORD

The work reported in this document was conducted by the Arnold Engineering Development Center under sponsorship of the National Aeronautics and Space Administration (NASA), Langley Research Center, Hampton, Virginia, for the Martin-Marietta Corporation, Denver Division, Denver, Colorado, under Program Element 921E-5.

The results of the test were obtained by ARO, Inc. (a subsidiary of Sverdrup & Parcel and Associates, Inc.), contract operator of the Arnold Engineering Development Center (AEDC), Air Force Systems Command (AFSC), Arnold Air Force Station, Tennessee. The tests were conducted on July 10 and 11, 1972, under ARO Project No. VA026; the final data analysis was completed on August 16, 1972. The manuscript was submitted for publication on October 3, 1972.

This technical report has been reviewed and is approved.

JIMMY W. MULLINS
Lt Colonel, USAF
Chief Air Force Test Director, VKF
Directorate of Test

A. L. COAPMAN
Colonel, USAF
Director of Test

CONTENTS

APPENDIXES

I. ILLUSTRATIONS

Figure

NOMENCLATURE

M_∞	Free-stream Mach number
p	Local surface pressure, psia
p_o	Tunnel stilling chamber pressure, psia
$p_{o'}$	Pitot pressure behind normal shock, psia
p_∞	Free-stream static pressure, psia
q_∞	Free-stream dynamic pressure, psia
R	Base cover radius, 6.003 in.
Re_R	Free-stream Reynolds number based on radius
S	Surface length from center of aeroshell to pressure tap (see Fig. 2a), in.
S^*	Surface length from center to edge of aeroshell (see Fig. 2a), in.
T_o	Tunnel stagnation temperature, °R
α	Model angle of attack, deg
β	Nondimensional parameter (see Fig. 5), $\alpha/(120° - \sigma_c)$
σ_c	Cone half angle, deg
ϕ	Angle around perimeter of model, deg
ψ	Model yaw angle, deg

SUBSCRIPTS

SP	Stagnation point

SECTION I
INTRODUCTION

The purpose of this investigation was to obtain surface pressure distributions on the Viking Lander Capsule (VLC) as a function of angle of attack. Items of particular interest were a verification of the vehicle base cover structural design using the measured pressure distribution, an assessment of the effects on the base cover pressure distribution of surface protuberances representing camera windows, control nozzles, etc., and comparisons of the aeroshell pressure distribution with measurements obtained in other facilities.

The tests were conducted in the 50-in. Hypersonic Wind Tunnel (C) of the von Karman Gas Dymanics Facility (VKF). Data were obtained at a nominal Mach number of 10 and Reynolds numbers based on the aeroshell radius of 0.28×10^6 and 0.79×10^6. Angle of attack was varied from -26 to 26 deg at each Reynolds number. Yaw angles of -5 and -10 deg were tested at approximately the trim angle of attack (11.2 deg). Shadowgraphs were obtained at each angle of attack, and oil flow pictures were made at a few selected test conditions.

SECTION II
APPARATUS

2.1 MODEL

The 8.73-percent-scale VLC model, supplied by Martin-Marietta Corporation, Denver Division, was fabricated from 304 stainless steel. A photograph of the model installed in the test section is presented in Fig. 1 (Appendix I). Model dimensions and the locations of the 90 pressure taps are given in Fig. 2a, and the protuberances located on the base cover of the model are described in detail in Fig. 2b, along with a table giving S/R and ϕ for each pressure tap location.

2.2 WIND TUNNEL

Tunnel C is a continuous, closed-circuit, variable density wind tunnel with a 50-in.-diam test section and a contoured axisymmetric nozzle that operates at a nominal Mach number of 10. The stilling chamber

pressure conditions range from 200 to 2000 psia at temperatures up to a maximum of 1900°R. The model can be injected into the test section for testing and retracted for cooling or changes without interrupting the tunnel flow.

SECTION III
TEST PROCEDURE

3.1 TEST CONDITIONS AND PROCEDURES

The test conditions were chosen to best simulate selected entry trajectories of the VLC into the Martian atmosphere. The high Reynolds number data represented the simulation of the estimated mean reentry trajectory, while the low Reynolds number data simulated a trajectory of minimum entry flight path angle. The two test conditions are listed below:

M_∞	p_O, psia	T_O, °R	p_∞, psia	q_∞, psia	$Re_R \times 10^{-6}$
10.07	1273.3	1888	0.0276	1.962	0.79
9.86	420.0	1891	0.0106	0.715	0.28

A complete summary of the test program is presented in Table I (Appendix II).

Because the model sting was offset from the aeroshell axis of symmetry, it was expected that model deflections would cause angle-of-attack changes large enough to require consideration in the data analysis. Pretest estimates of these deflections were made, and the tunnel sector angle of pitch was changed accordingly in the test program. The actual model angle of attack was determined by measuring the angle of the aeroshell surface relative to horizontal reference lines provided in the shadowgraph obtained for each test attitude. A typical shadowgraph illustrating this technique is presented in Fig. 3. The angles of attack listed in Table I are the measured values.

The test procedure used was to inject the model at nominally zero angle of attack and adjust the sector pitch angle until the readings from

pressure tap pairs 2 & 18 and 3 & 15, located at equal but opposite distances from the center of the aeroshell, indicated the same pressure. This attitude was selected as zero angle of attack, and all other angles were referenced to it. Corresponding pressure taps in the yaw plane were monitored and indicated little or no yaw of the model.

Tests for the negative angle-of-attack series required that the model be rotated 180 deg with respect to the tunnel support system. The procedure of matching the pressures at opposite taps on the aeroshell was repeated, and small adjustments were made to define again the model zero angle of attack.

During the oil flow tests, difficulties were encountered in getting the oil to perform properly. The resulting oil flow photographs were not as good as expected, mainly because the aeroshell heated up rapidly, thereby inhibiting the oil flow. On the model base cover the surface shear was too low to cause even a very low viscosity oil to flow in a regular pattern. For these reasons none of the oil flow pictures are presented for discussion.

A stress analysis revealed that the maximum temperature which the model could reach and stay within the required stress limitations was 1200°F. Therefore, two Chromel®-Alumel® thermocouples were installed in the interior of the model to monitor the bulk material temperature.

Model flow-field shadowgraphs were obtained at all test conditions using a parallel-beam refocused shadowgraph system.

3.2 INSTRUMENTATION AND PRECISION

Tunnel C stilling chamber pressure is measured with 500- and 2500-psid transducers referenced to a near vacuum. Based on periodic comparisons with secondary standards, the uncertainty (a bandwith which includes 95 percent of the residuals) of these transducers is estimated to be ±0.2 percent of the calibrated range. Stilling chamber temperature is measured by a Chromel-Alumel thermocouple with an uncertainty of ±1.0 percent based on the thermocouple wire manufacturer's specifications. These uncertainties, along with the calibrated uniformity of the tunnel test section flow which gives the uncertainty in Mach number as ±0.3 percent, were used to estimate the following free-stream properties by use of the Taylor series method of error propagation:

$Re_R \times 10^{-6}$	Uncertainties, percent						
	M_∞	T_o	p_o	p_o'	p_∞	q_∞	Re_R
0.28	±0.3	±1.0	±0.3	±0.5	±2.0	±1.4	±0.5
0.79	±0.3	±1.0	±0.4	±0.6	±2.0	±1.5	±0.5

The uncertainties in the measured data were obtained by combining the precision of the surface pressure transducers and those calculated for the tunnel parameters in a similar application of the Taylor series method of error propagation. If the measured pressure was in the range $1.0 < p < 15.0$, it was measured on the 15-psid transducer with an uncertainty of ±0.015 psia. If the pressure was less than 1.0 psia, it was measured on the 1-psid transducer. This transducer has five ranges which further divide the pressure measurements to give better accuracy. These ranges are listed below, along with the associated precision for each range.

Range, psia		Error	Minimum ±Percent
From	To	± psia	Error
0.3	1.0	0.01	1.0
0.1	0.3	0.003	1.0
0.03	0.1	0.001	1.0
0.01	0.03	0.0003	1.0
0.003	0.01	0.0002	2.0

Some typical measured pressures for these tests and associated uncertainties in p and p/p_o' are shown below:

$Re_R \times 10^{-6}$	Nominal Pressure, psia	Uncertainties, percent	
		p	p/p_o'
0.79	3.60	±0.4	±0.6
0.79	0.132	±2.3	±2.3
0.28	0.00464	±4.3	±4.3

SECTION IV
RESULTS AND DISCUSSION

Summary plots of the pressure distribution in the model vertical plane of symmetry obtained during these tests are presented in Figs. 4a through g for all the angles of attack tested. No Reynolds number effect was observed for these data, so only data for $Re_R = 0.79 \times 10^6$ are presented. The distributions for the model at both the positive and the negative angles of attack are presented except those for $\alpha = 0$ deg from the negative angle-of-attack series and $\alpha = 26$ deg from the positive angle-of-attack series (reasons for omission of these data are given later).

In most cases the distributions from the positive and negative angle-of-attack series compliment each other very well. The discrepancy ($p/p_0' > 1.0$) of the pressures in the stagnation region of the distributions for $\alpha = 8$ and 12 deg (Figs. 4c and d) was caused by a localized change in the flow Mach number; agreement of the distributions over the rest of the model surface confirms this. Hence, for these two cases the distribution in the stagnation region indicated by the negative angle-of-attack data is preferable.

One of the main reasons for testing the symmetrical model at both positive and negative angles of attack was to determine if the offset sting has any influence on the base cover distributions, particularly whenever the sting was exposed to the windward flow. The data shown in Figs. 4a through g for $|S/R| \geq 1.1$ correspond to orifice locations from the model shoulder to the center of the base cover in the pitch plane, so comparison of the distributions for these data at positive (sting windward) and negative (sting leeward) angles of attack is a measure of this effect. The data shown are plotted at ten times the actual value, and it is evident that the sting position had little effect.

The positive and negative angle-of-attack distributions on the leeward side of the aeroshell (positive S/R) agree very well except for the $\alpha \approx 20$-deg case (Fig. 4f). This difference was caused by model bow shock-tunnel boundary-layer interaction which caused the pressures in this region to increase. The interaction at $\alpha \approx 26$ deg was so severe that the data were omitted from the report (as stated earlier); however, the data for $\alpha \approx 20$ deg were retained to show the beginning of this anomaly. The distributions in this region for $\alpha \approx -20$ and -26 deg should be taken as representative of these conditions. The model was located further

from the tunnel wall for the negative angles of attack than for the positive angles; hence, the absence of interaction effects at α = -20 and -26 deg. The data on the windward side of the aeroshell for $\alpha \approx 20$ and 26 deg appear uninfluenced and have been retained. The data for $\alpha \approx 0$ of the negative angle-of-attack series were excluded because the shadowgraphs show the model to be at an angle of attack of about -0.5 deg, which precludes any comparison with the α = 0-deg data.

Shown also in Fig. 4 are indicated stagnation points for each angle of attack selected as the point at which the pressure ratio is maximum. In some cases a single point could not be selected, so a region was indicated to show the limits on the stagnation point location. Reference 1 presents an extensive treatment of large angle conical bodies of the VLC configuration type for supersonic and low hypersonic Mach numbers and includes a correlation of the stagnation point location with angle of attack. This correlation compared with the selected points for these data is presented in Fig. 5. Good agreement is evident, indicating little or no free-stream Mach number effect in this regard since the correlation is based on data at Mach 2.3 to 4.63.

An assessemnt of the influence of the protuberances on the base cover pressure distribution is presented in Figs. 6 and 7. Figure 6 shows the pressure distribution at $\alpha \approx 0$ along the 315-deg meridian as a reference compared with the values from the pressure orifices surrounding the protuberances. Similar comparisons are shown in Fig. 7 at angle of attack for the camera bump and reaction control system (RCS) block (the bridle and antenna were omitted because at angle of attack only data at the same radial angles are comparable). It appears that in all cases the presence of the protuberances had little or no effect on the base cover pressure distribution.

Finally, comparisons are presented in Fig. 8 which show the expected absence of Mach number effect between M_∞ = 8 and 10 on the VLC aeroshell pressure distribution. In addition, results from separate facilities (Mach 8 results from NASA/Langley provided by Martin-Marietta Corporation, Denver, Ref. 2) are in good agreement.

SECTION V
CONCLUSIONS

Pressure tests were made on the NASA/Martin Viking Lander Capsule at Mach number 10 and Reynolds numbers, based on model base cover radius, of 0.28×10^6 and 0.79×10^6. Within the limits of the test scope the significant results were as follows:

1. Pressure distributions obtained on the model front face with the model offset sting windward compared with those for the sting leeward showed no effect of the sting presence throughout the test angle-of-attack range. Similar results were obtained for the distributions on the base cover half area above the sting location (only region instrumented).

2. Stagnation point location as a function of angle of attack agreed well with a correlation developed for Mach numbers ≤ 5, indicating little Mach number effect on this phenomenon up to $M_\infty = 10$.

3. Presence of the protuberances representing camera locations, antennae, etc., on the model base cover had no measurable effect on the surrounding pressure distributions.

REFERENCES

1. Campbell, James F. and Tudor, Dorothey H. "Pressure Distributions on 140°, 160°, and 180° Cones at Mach Numbers from 2.30 to 4.63 and Angles of Attack from 0° to 20°." NASA TN D-5204, May 1969.

2. Faye-Peterson, R., Sarver, D., and Carroll, H. "Heat Transfer and Pressure Distributions at M = 8 on 0.029 Scale Models of the Viking Entry Vehicle." Report TP-3720318, Martin-Marietta Corp., Denver Division, July 1972.

APPENDIXES

I. ILLUSTRATIONS

II. TABLES

Preceding page blank

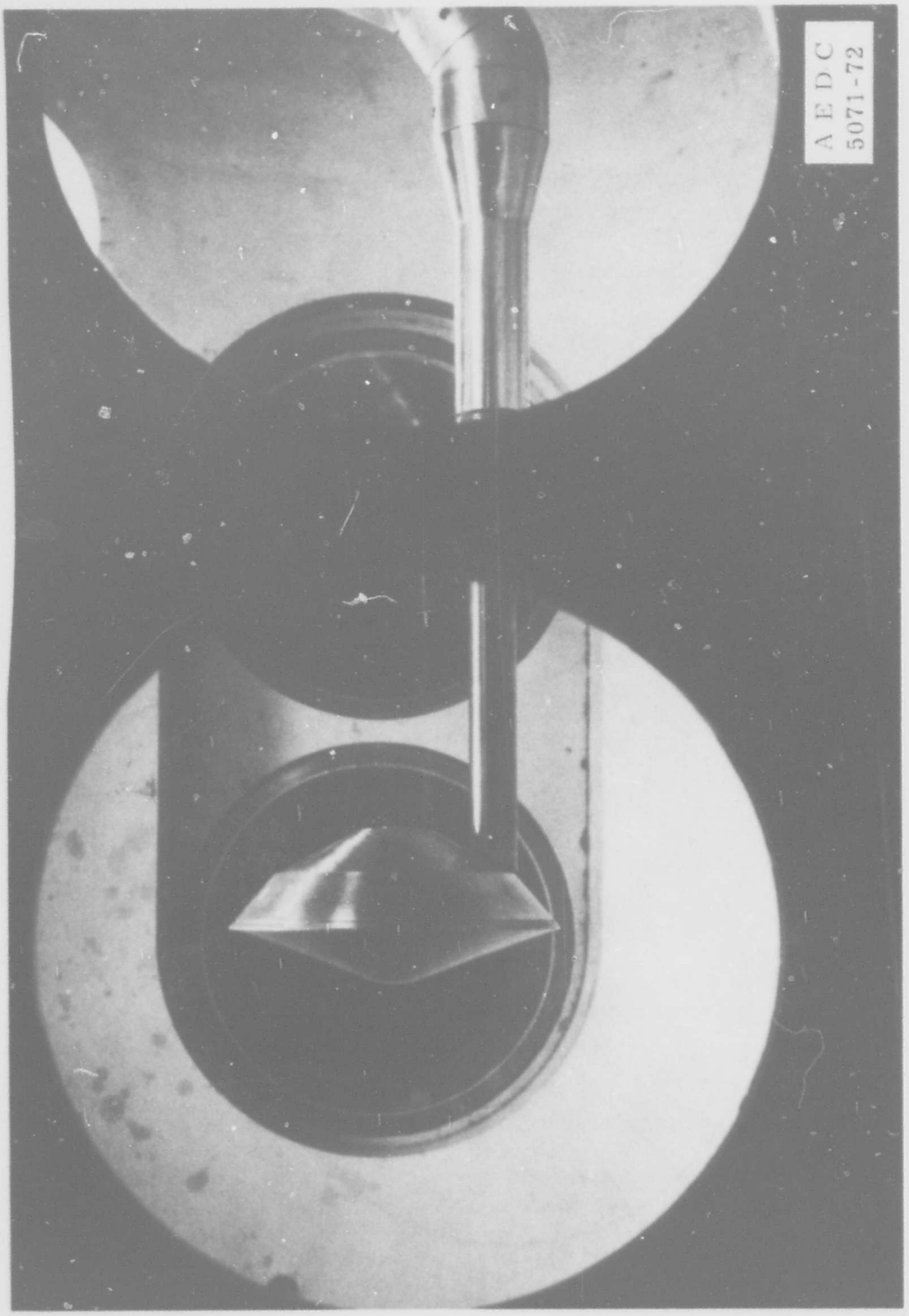

Fig. 1 Photograph of Model in Tunnel C Test Section

Preceding page blank

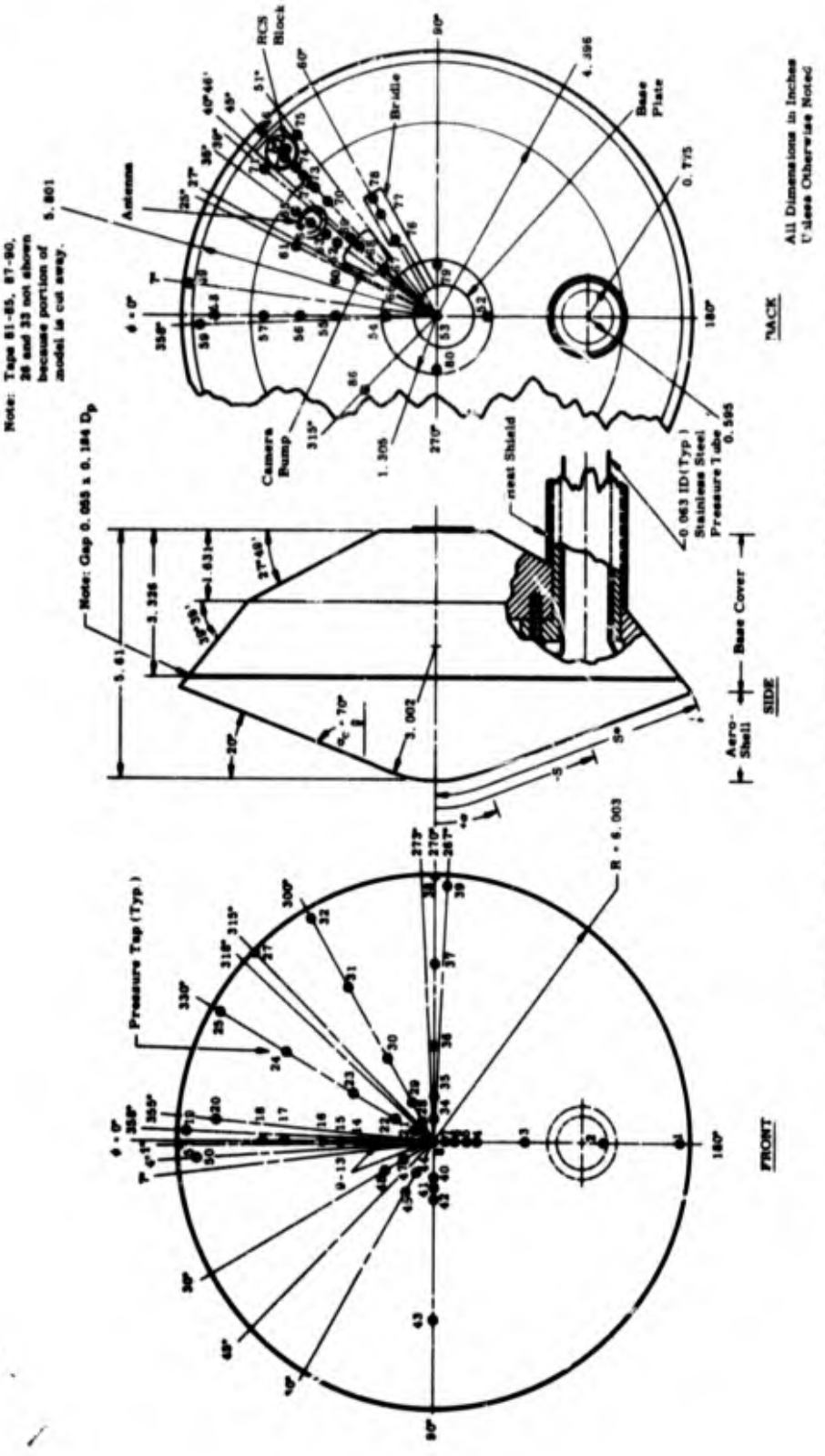

a. Model Dimensions and Pressure Tap Locations

Fig. 2 Model Dimensions, Pressure Tap Locations, and Base Cover Protuberance Details

Tap No.	ϕ	S/R
1	180°	-1.0222
2		-0.7392
3		-0.3781
4		-0.1745
5		-0.1309
6		-0.0873
7	180°	-0.0436
8	---	0.0000
9	0°	0.0436
10		0.0873
11		0.1309
12		0.1745
13		0.2239
14		0.3010
15		0.3781
16		0.4552
17		0.6095
18	0°	0.7392
19	358°	1.0222
20	355°	0.9025
21	330°	0.0873
22		0.1745
23		0.3781
24		0.7392
25	330°	1.0222
26	318°	1.0910
27	315°	1.0643
28	300°	0.0873
29		0.1745
30		0.3781
31		0.7392
32	300°	1.0222
33	273°	1.0910
34	270°	0.0873
35		0.1745
36		0.3781
37		0.7392
38	270°	1.0643
39	267°	1.0222
40	90°	0.1309
41		0.1745
42		0.2239
43	90°	0.7392
44	60°	0.1309
45	60°	0.2239

Tap No.	ϕ	S/R
46	45°	1.0910
47	30°	0.1309
48	30°	0.2239
49	7°	1.0910
50	4°	0.8796
51	1°	1.0643
52	180°	-2.0784
53	---	2.2886
54	0°	2.0784
55		1.9151
56		1.7147
57		1.5490
58	0°	1.2719
59	358°	1.1784
60	27°	1.9151
61	25°	1.6319
62	35°	1.7772
63		1.7147
64		1.6319
65	35°	1.5490
66	40°46'	2.0784
67		2.0104
68		1.9151
69	40°46'	1.8196
70	45°	1.6319
71	39°	1.2719
72	45°	1.5490
73	45°	1.4729
74	45°	1.3946
75	51°	1.2719
76	60°	1.9543
77	60°	1.8196
78	60°	1.7594
79	90°	2.0784
80	270°	2.0784
81		1.9151
82		1.7147
83		1.5490
84	270°	1.2719
85	268°	1.1784
86	315°	1.9151
87		1.7147
88		1.5490
89	315°	1.2719
90	313°	1.1784

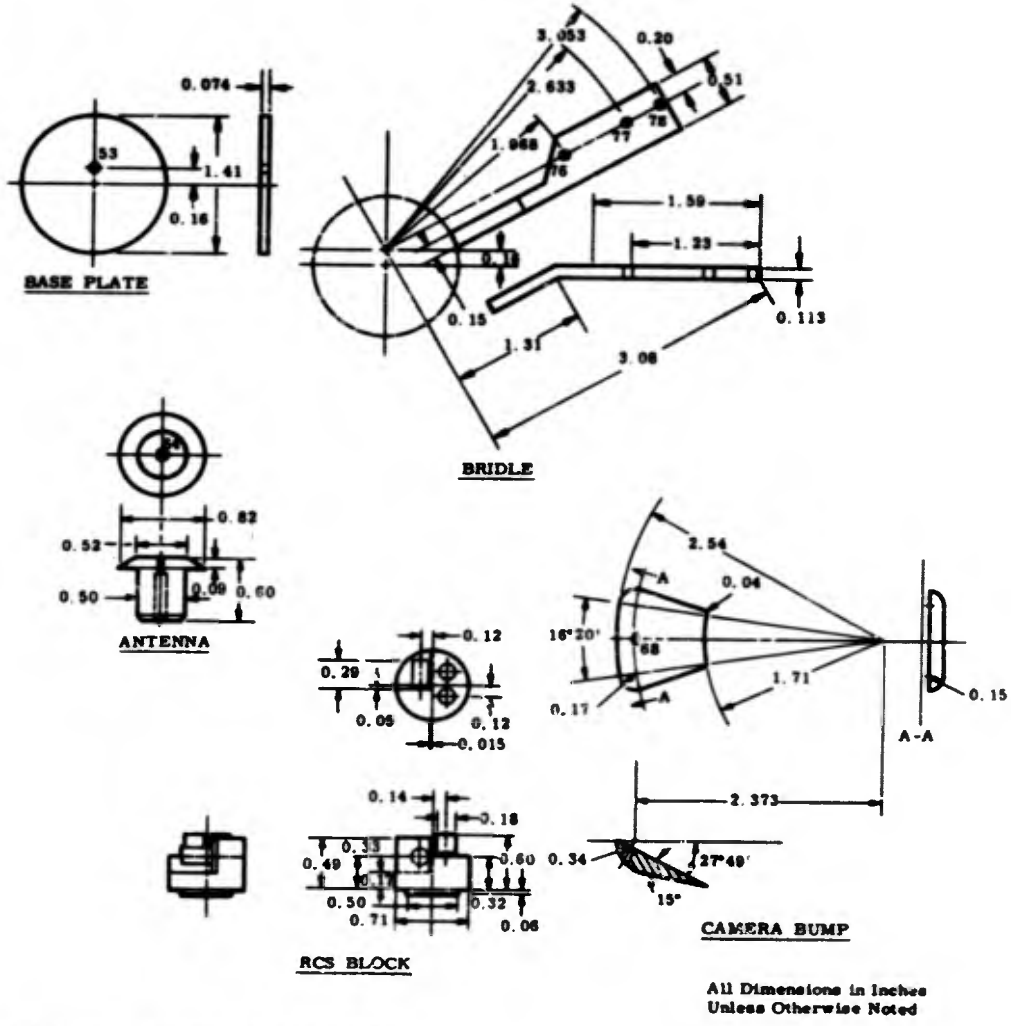

b. Base Cover Protuberance Details

Fig. 2 Concluded

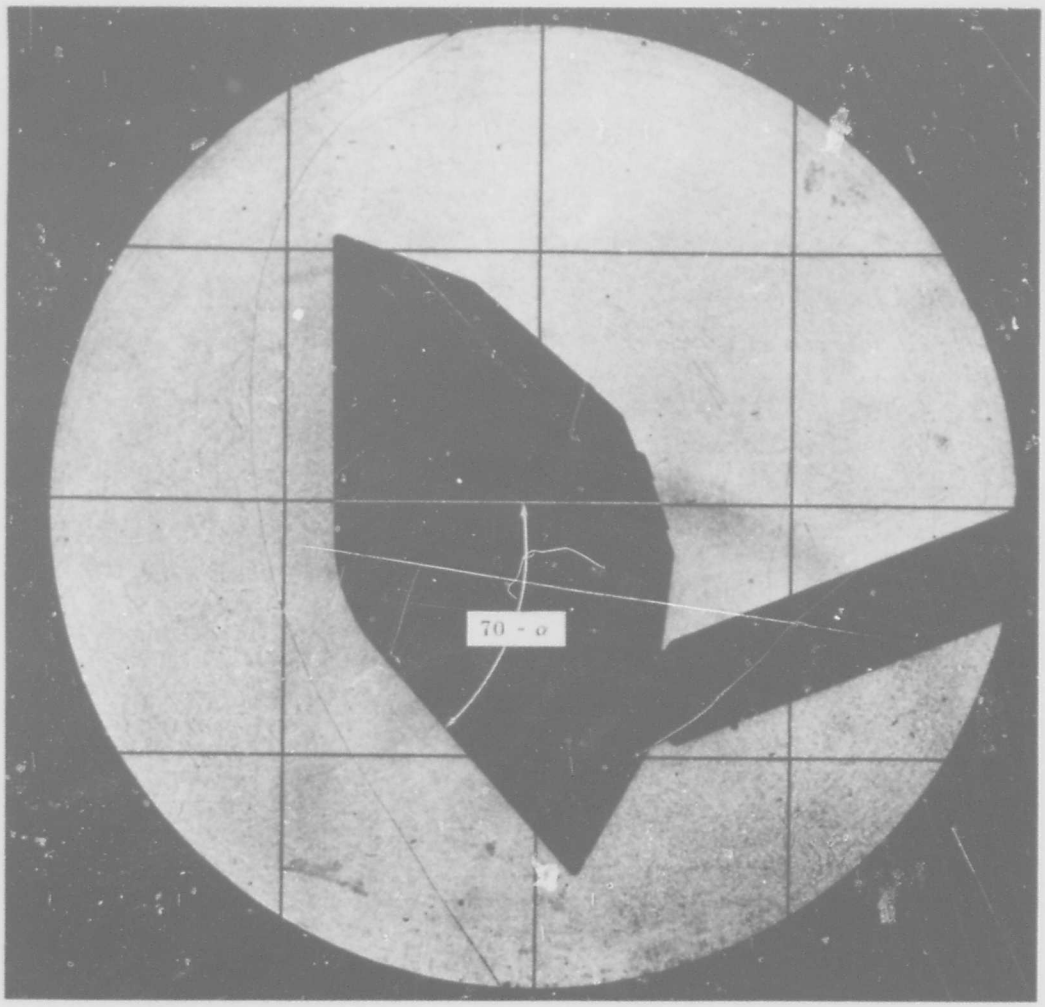

Fig. 3 Shadowgraph Showing Model Angle-of-Attack Determination, α = 20 deg, $M_\infty \approx 10.06$, $Re_R \approx 0.79 \times 10^6$

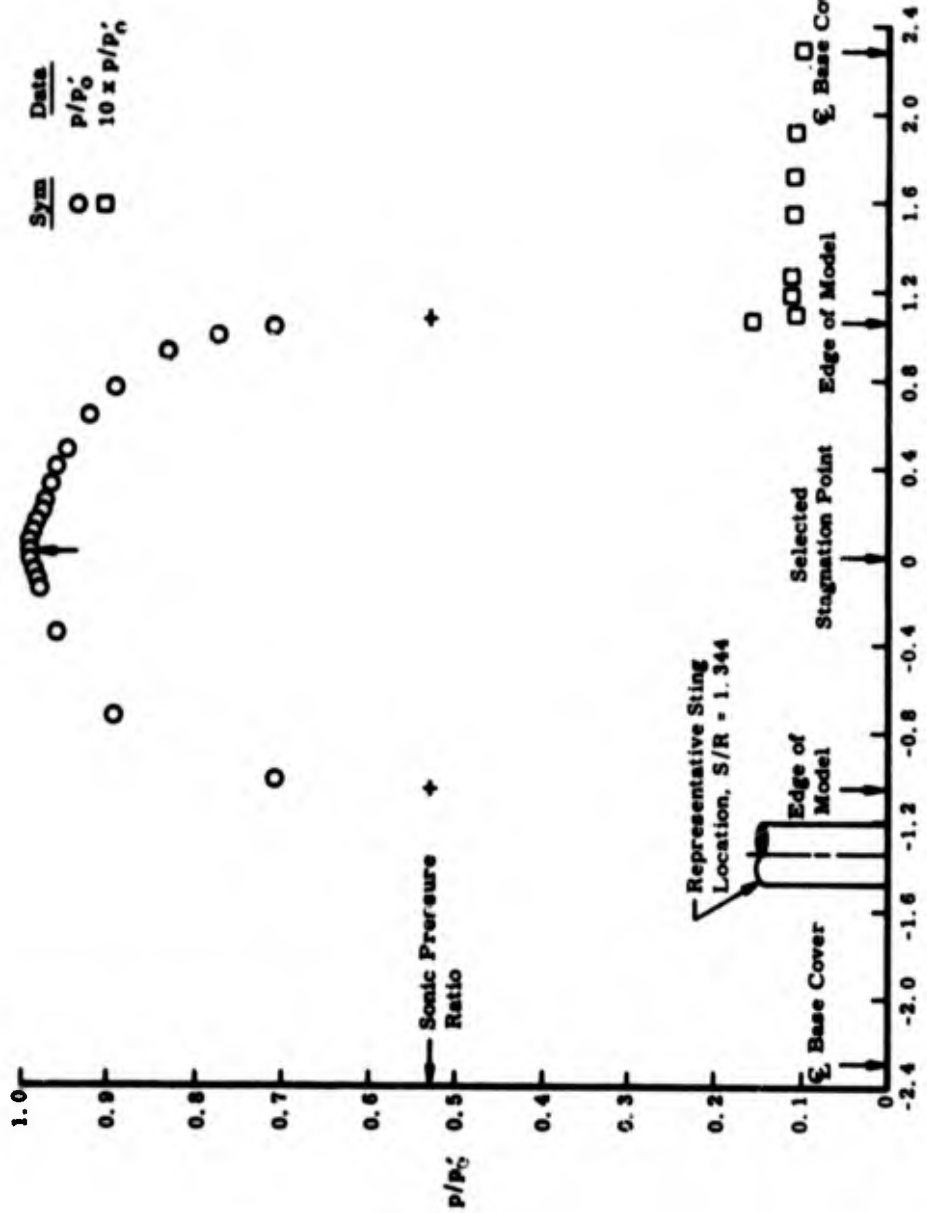

Fig. 4 Pressure Distribution Along the Vertical Plane of Symmetry at Several Angles of Attack, $M_\infty = 10$, $Re_R = 0.79 \times 10^6$

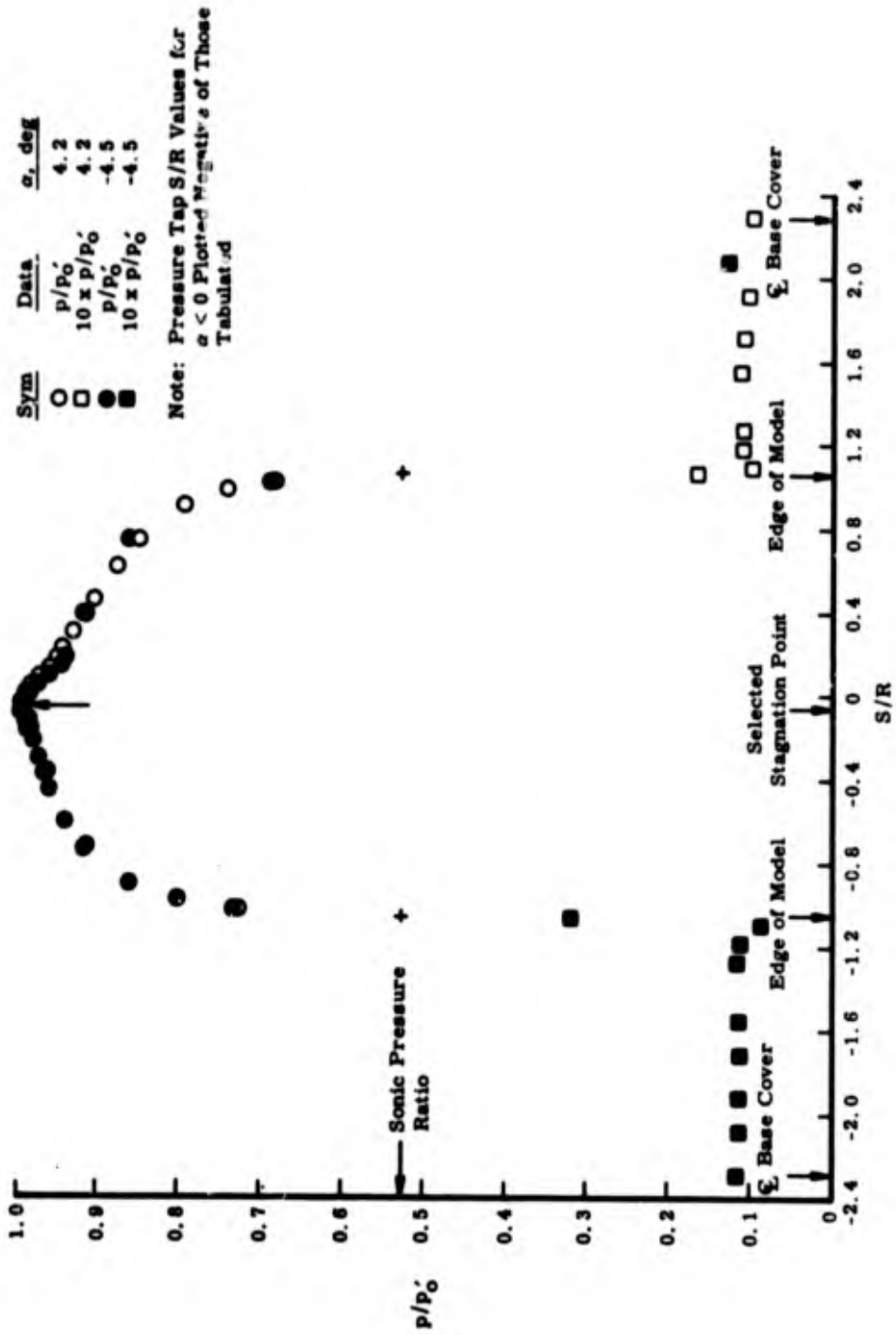

b. α = 4.2 and -4.5 deg
Fig. 4 Continued

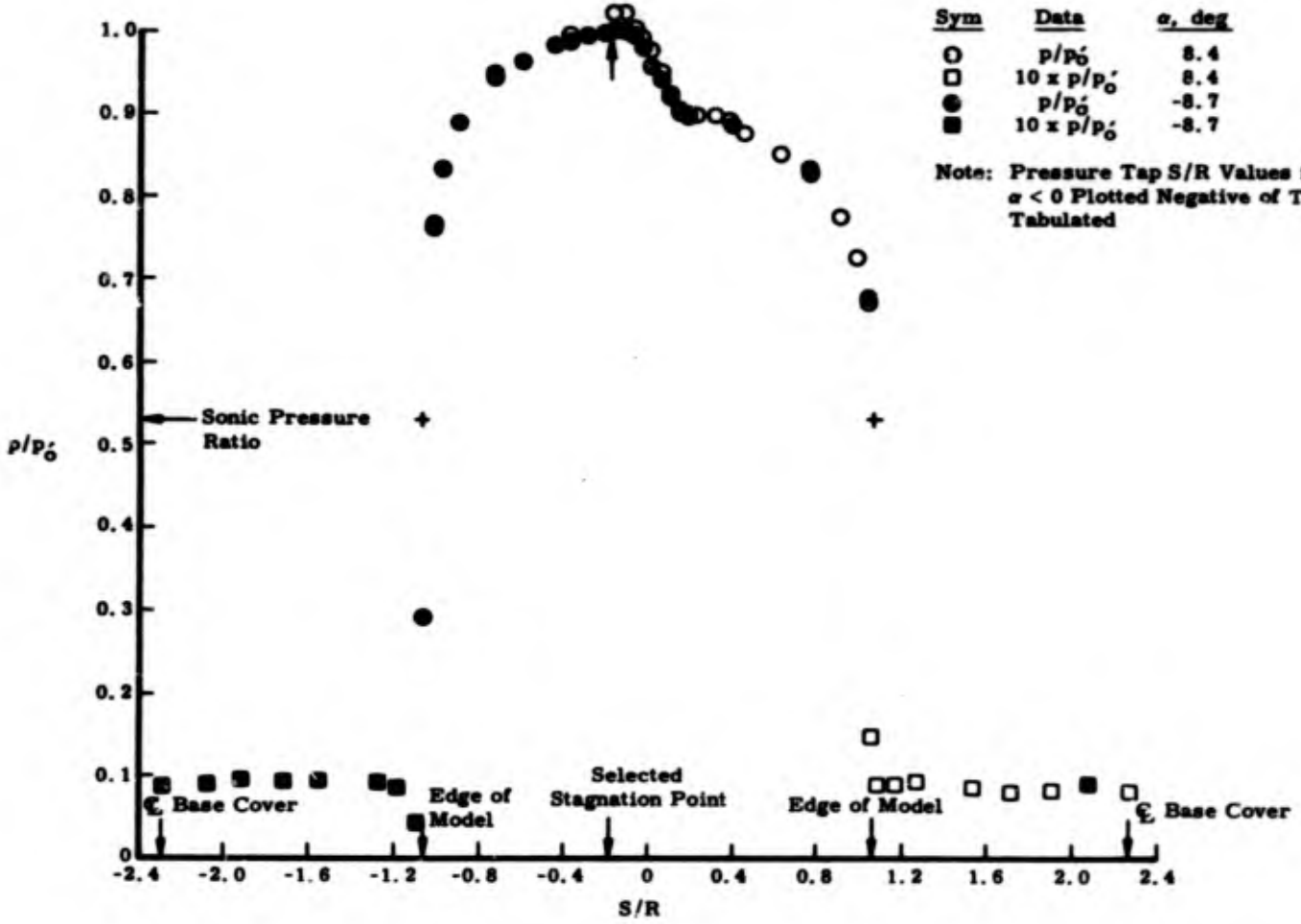

c. α = 8.4 and -8.7 deg

Fig. 4 Continued

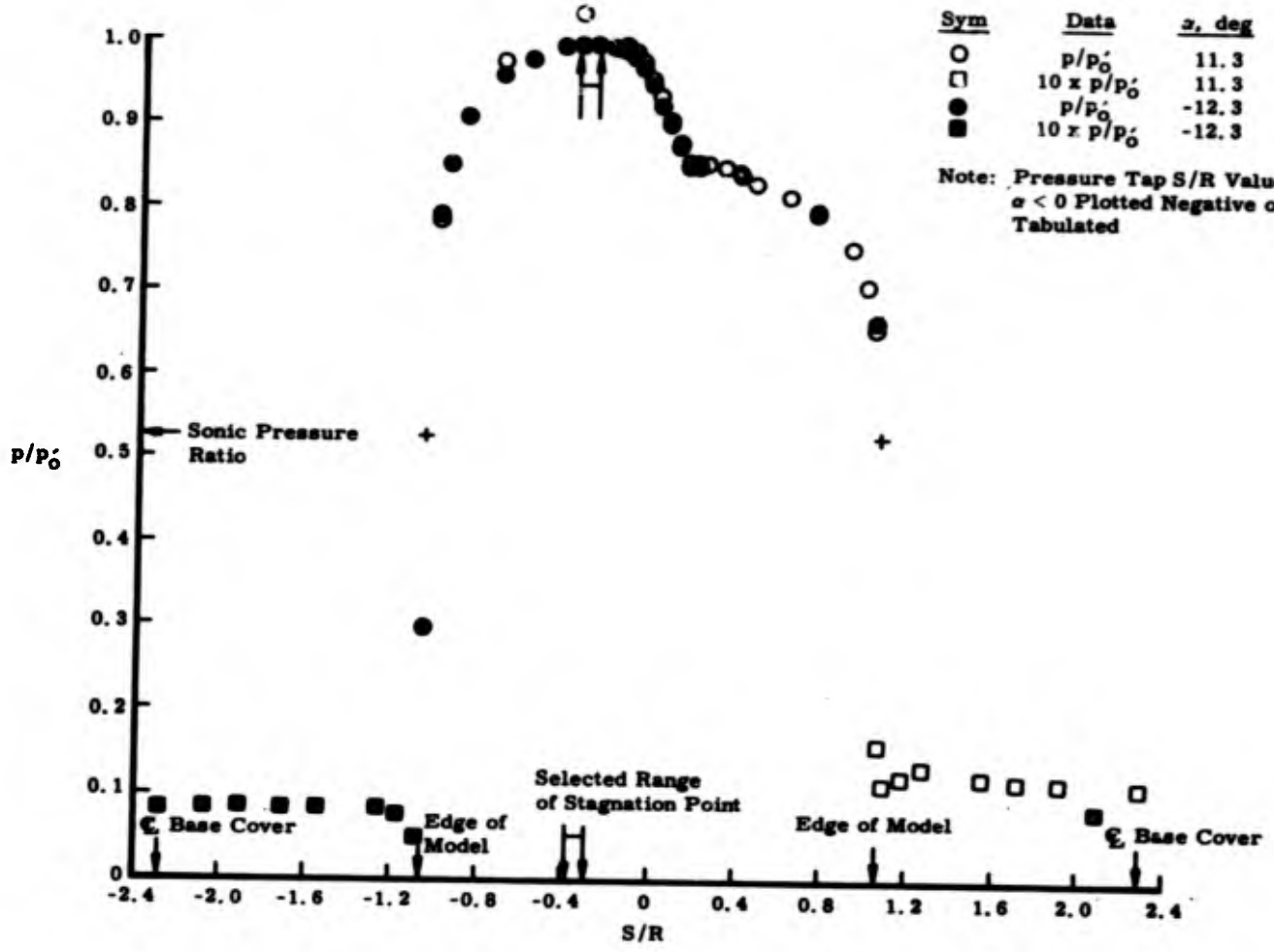

d. α = 11.3 and -12.3 deg

Fig. 4 Continued

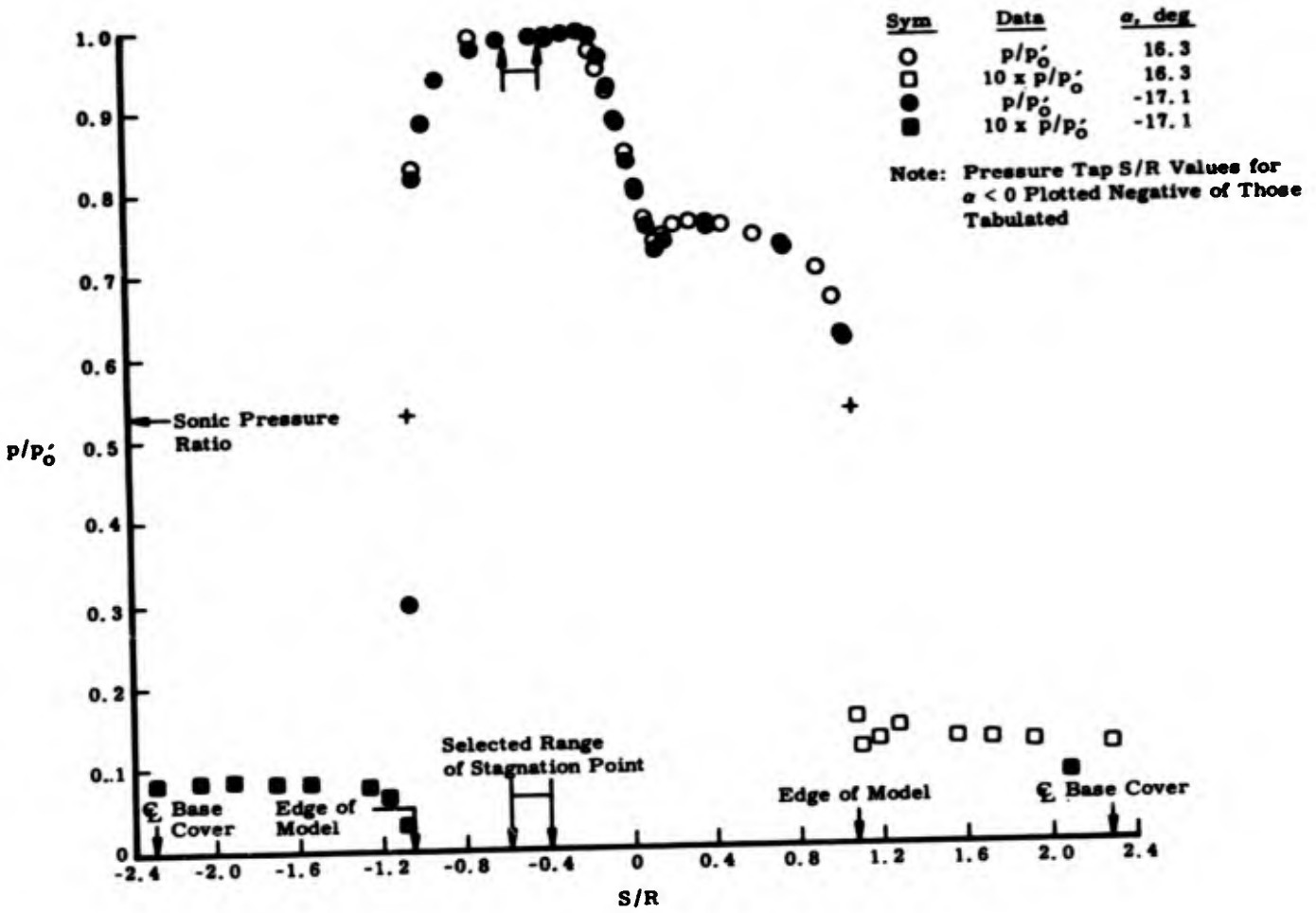

e. α = 6.3 and -17.1 deg

Fig. 4 Continued

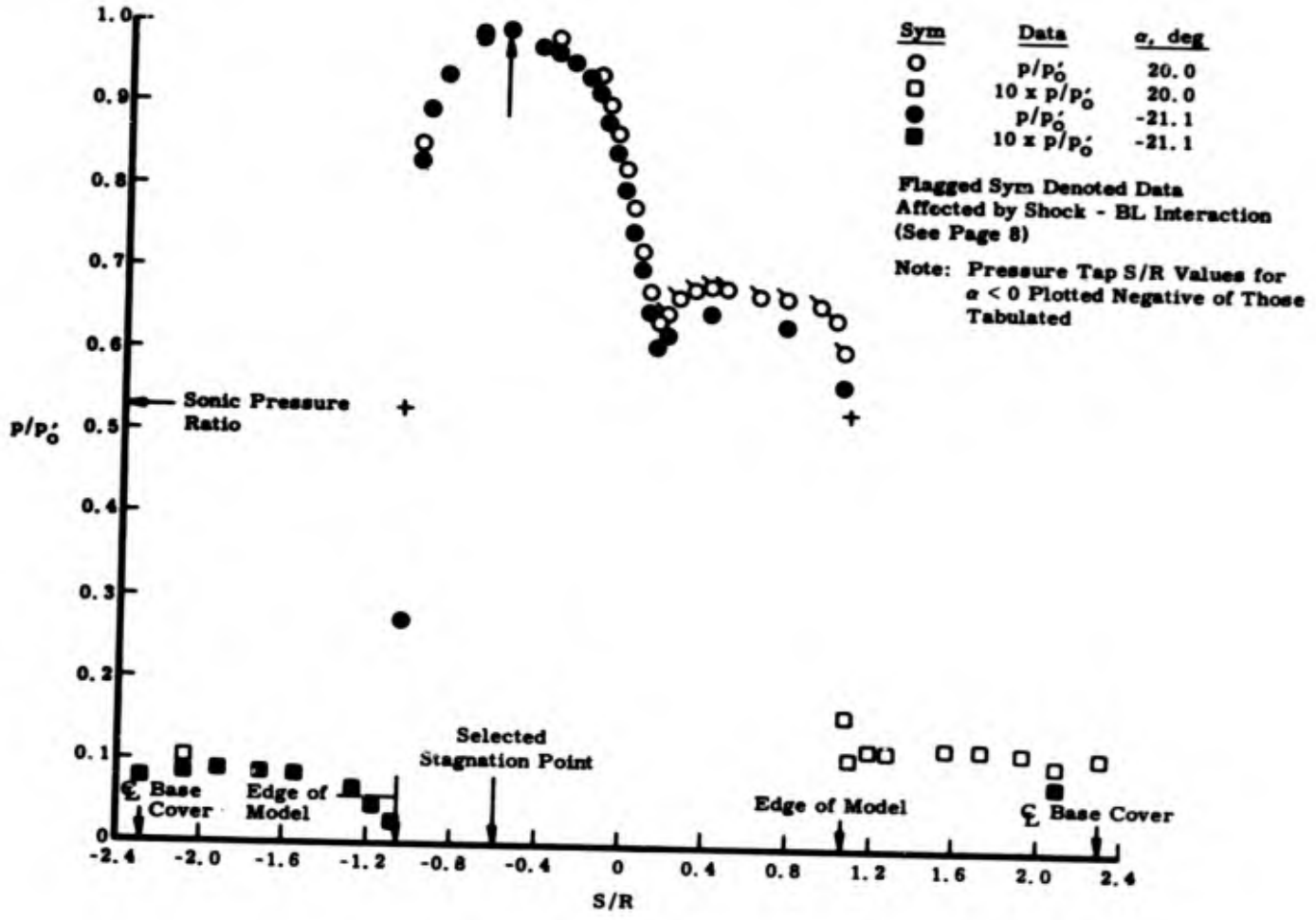

f. α = 20.0 and -21.1 deg
Fig. 4 Continued

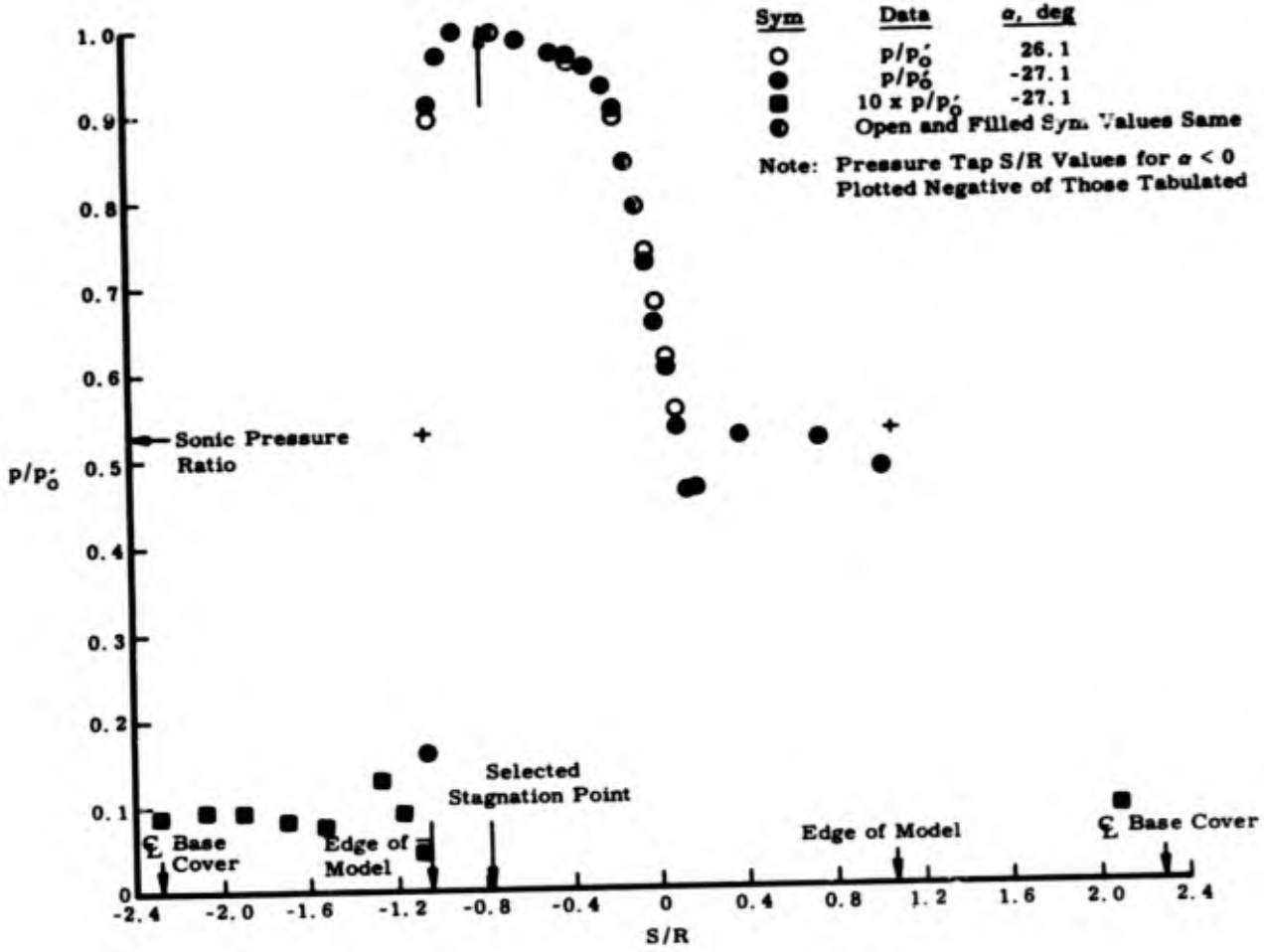

g. α = 26.1 and -27.1 deg
Fig. 4 Concluded

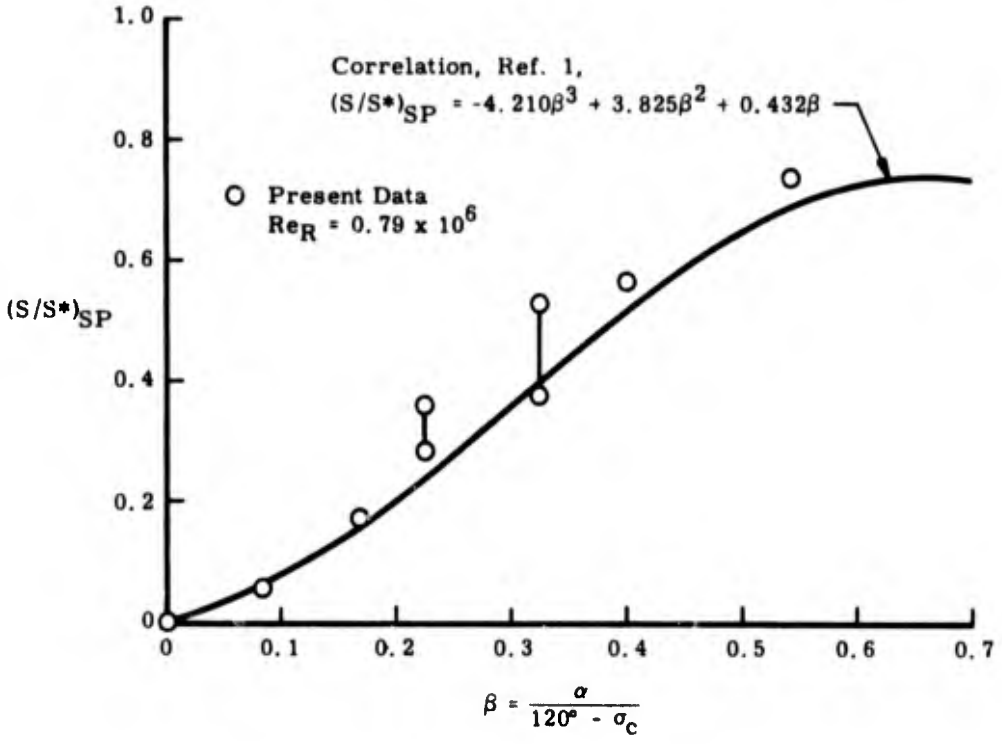

Fig. 5 Comparison of Observed Stagnation Point Location on VLC Aeroshell with Theory for Test Angles of Attack, σ_c = 70 deg

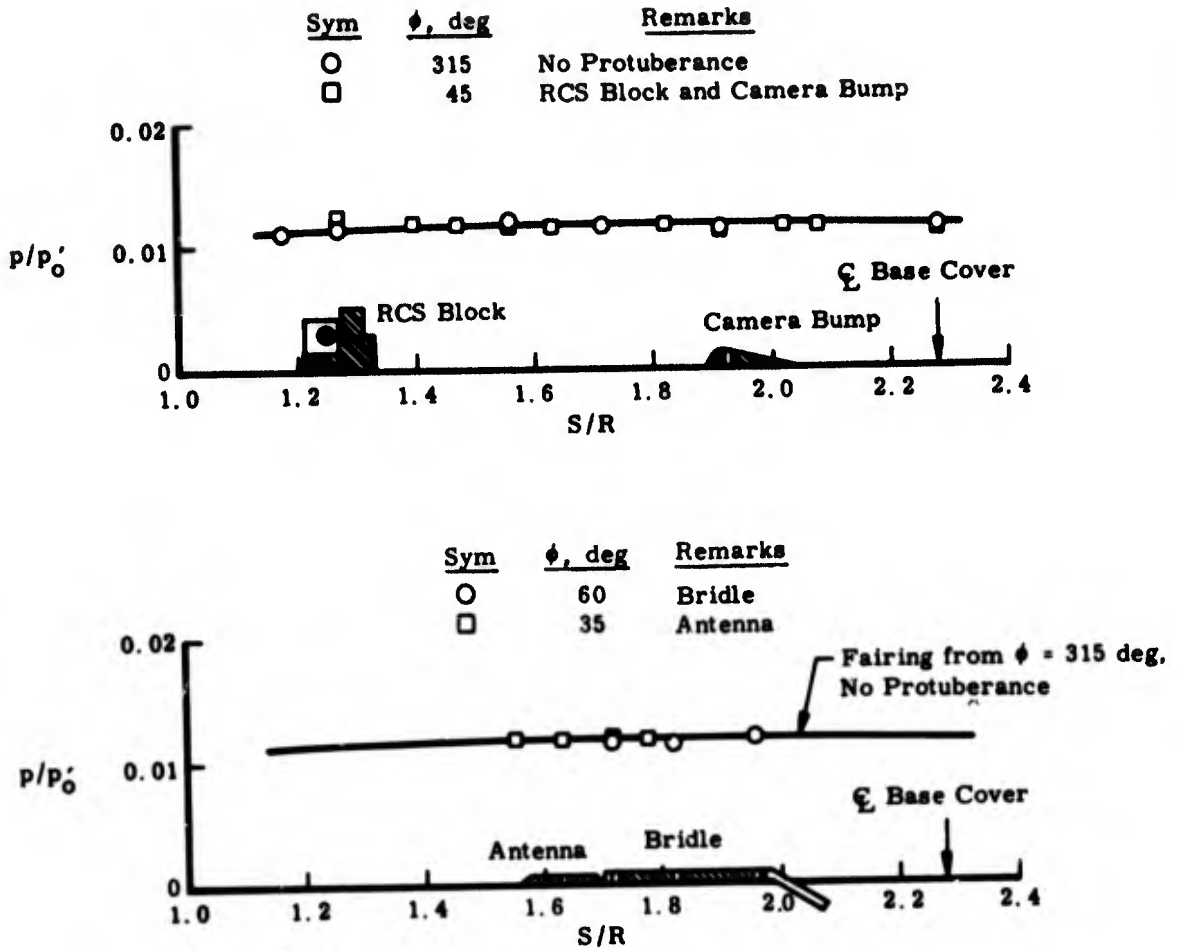

Fig. 6 Effects of Protuberances on Pressure Distribution Over Model Base Cover at $\alpha = 0$, $Re_R = 0.79 \times 10^6$

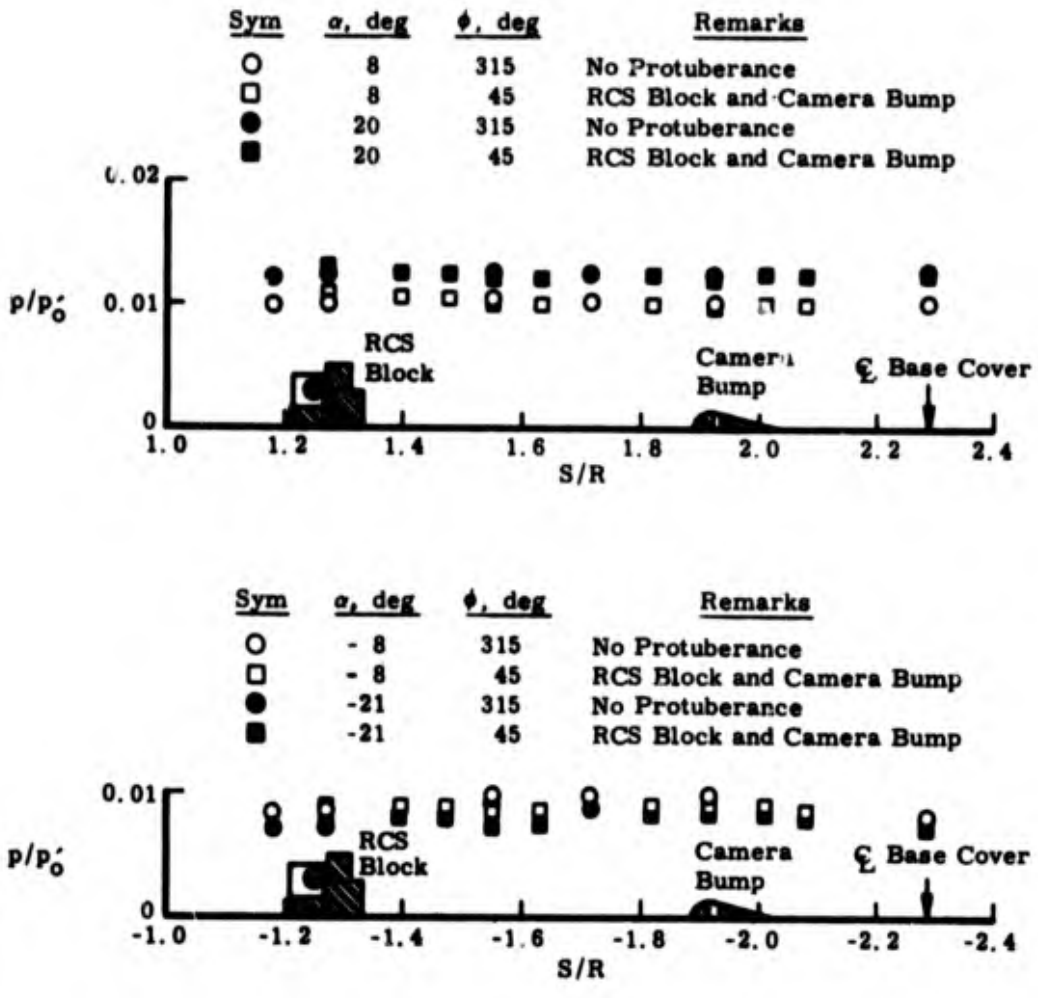

Fig. 7 Effects of Protuberances on Pressure Distribution Over Model Base Cover at Several Angles of Attack, $Re_R = 0.79 \times 10^6$

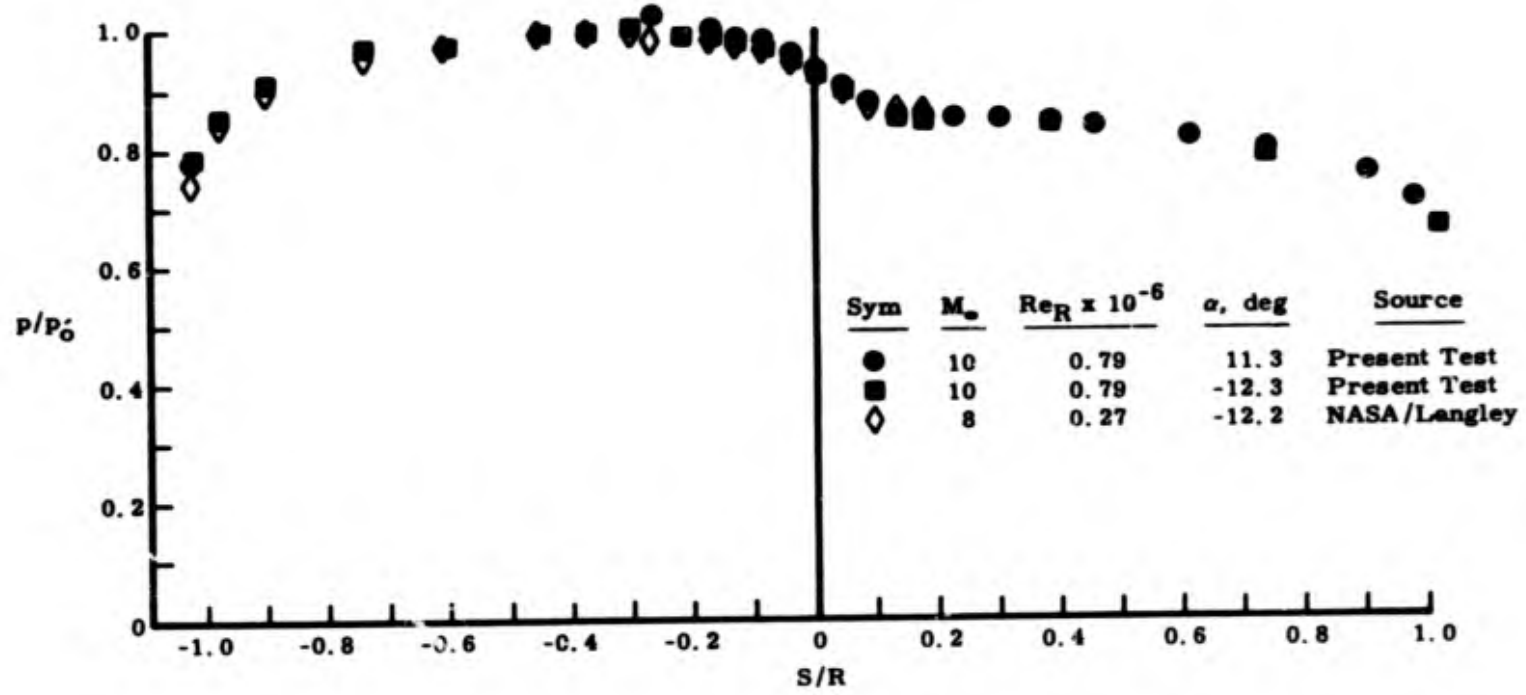

a. $\alpha \approx 12$ deg

Fig. 8 Comparisons of Pressure Distribution on VLC Aeroshell at Mach Numbers 8 and 10 for α = 12 and 20 deg

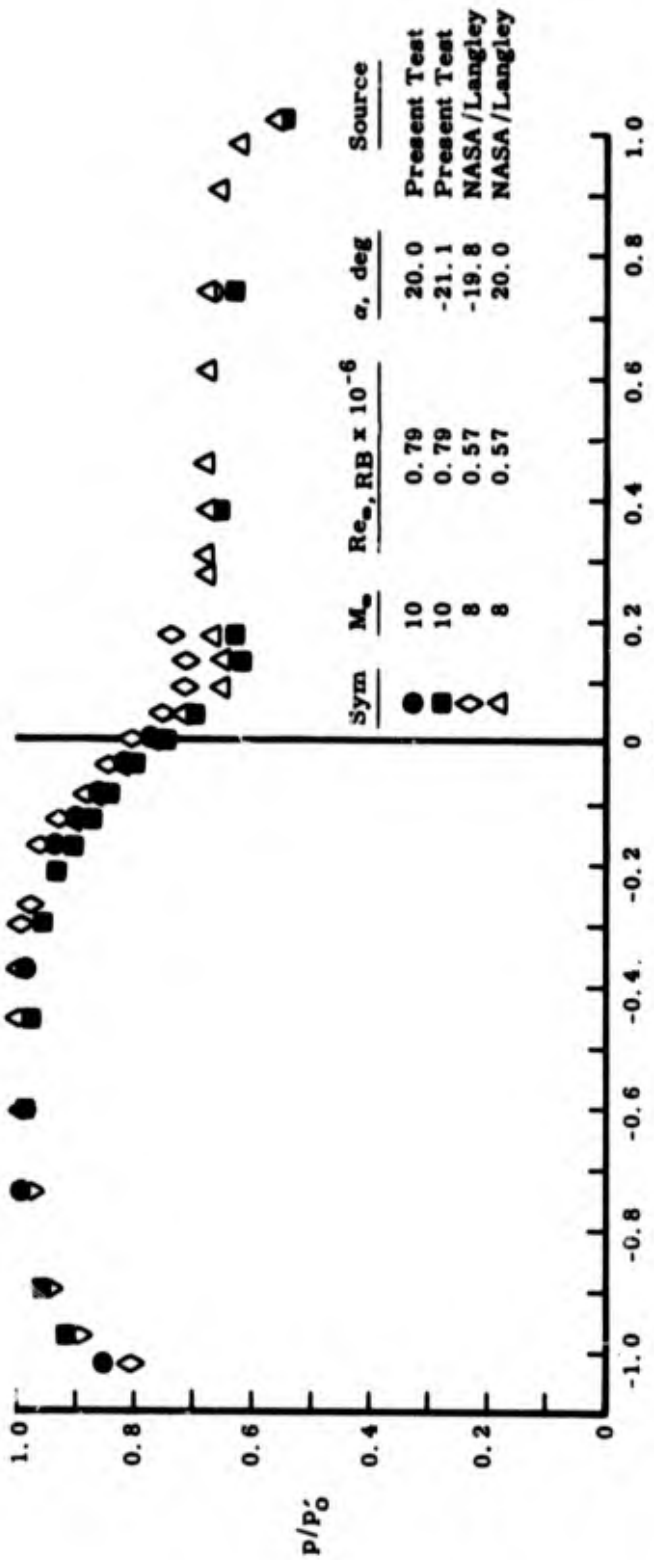

b. $\alpha \approx 20$ deg
Fig. 8 Concluded

TABLE I
TEST SUMMARY

M_∞	$Re_R \times 10^{-6}$	α, deg	ψ, deg
10.07	0.79	0.3	0
		-0.5	
		-0.63	
		4.2	
		-4.5	
		8.4	
		-8.7	
		11.3	
		-12.3	
		16.3	
		-17.1	
		20.0	
		-21.1	
		26.1	
		-27.1	
		-27.4	
9.86	0.28	-0.1	
		-0.8	
		4.0	
		-5.3	
		8.1	
		-9.3	
		11.4	
		-12.4	
		16.3	
		-17.3	
		20.3	
		-21.1	
		22.4	
		-23.1	
		-25.0	
		26.4	
		-27.1	
		-27.3	(Model sting diameter increased by 1.0 in.)
		-21.3	
		11.4	-10.0
		11.3	-5.0